Modeling Electrical Field Distribution
in Layered Geological Rock Formations
with a Borehole Using the Coulomb Charges Method

Adam CICHY and Andrzej OSSOWSKI

AGH University of Science and Technology,
Department of Geology, Geophysics and Environmental Protection,
Kraków, Poland; e-mails: cichy@agh.edu.pl, ossowski@geol.agh.edu.pl

A b s t r a c t

The Coulomb charges method is used to model apparent resistivity measurements carried out in layered geological formations with a borehole using various devices. It is characterized by a high level of effectiveness and accuracy. The results are compared with the theoretical solutions for a homogenous medium with the borehole and invaded zone for point current source lateral devices. The relative error was less than 2% for different values of the range of the invaded zone and resistivity of invaded and true resistivity of formation.

Key words: Coulomb charges method, apparent resistivity, lateral device, normal device.

1. INTRODUCTION

Modeling borehole geophysical tools which measure the apparent resistivity is very important in order to determine the true resistivity of a rock formation. Currently, the finite element method is mainly used for this purpose (Tan *et al*. 2011). Calculations using this method are time-consuming and require powerful computers. For such a type of modeling, the Coulomb charges method can be used (Alpin 1964, Alpin *et al*. 1985). The algorithm

proposed in this paper has been modified from algorithms published previously and shows a high degree of effectiveness and accuracy. It is also much less time-consuming and calculations can be carried out on an ordinary PC.

2. THEORETICAL BASIS

The Coulomb charges method (Alpin 1964, Alpin *et al.* 1985) can be used to solve the first kind of boundary problem for the Lapalace equation with internal boundary conditions by reducing it to the Fredholm integral equations of the second kind. The algorithm presented here assumes a rock formation model consisting of horizontal homogenous layers with a vertical borehole as well as vertical cylindrical coaxial homogenous layers with diameters reflecting the ranges of invaded zones. Horizontal and vertical layers can be of different thickness and resistivity. The idea of the Coulomb charges method is as follows (Alpin 1964, Alpin *et al.* 1985):

At the boundary between two conducting media with different resistivity, the normal component of current density vector is continuous. At each point "p" laying on the surface separating two media we have the following relation:

$$\frac{1}{R^i} \cdot E_n^i(\mathrm{p}) = \frac{1}{R^{i+1}} \cdot E_n^{i+1}(\mathrm{p}) \; , \tag{1}$$

where R^i and R^{i+1} are the resistivities of two homogenous media with numbers i and $i+1$; and $E_n^i(\mathrm{p})$ and $E_n^{i+1}(\mathrm{p})$ are the normal components of the electrical field at point "p".

The normal component of the electrical field, E_n, can be explained by the presence of surface charge density $\sigma(\mathrm{p})$. The dependence between the surface charge density and normal components of electrical field at point "p" is expressed by the following relation:

$$E_n^{i+1}(\mathrm{p}) - E_n^i(\mathrm{p}) = \frac{\sigma(\mathrm{p})}{\varepsilon_0} \; , \tag{2}$$

where ε_0 is the permittivity of vacuum.

Transforming Eqs. 1 and 2 we obtain the following relation (Alpin 1964, Alpin *et al.* 1985):

$$\sigma(\mathrm{p}) = 2\varepsilon_0 K(\mathrm{p}) E_n^{\mathrm{av}}(\mathrm{p}) \; , \tag{3}$$

where $K(\mathrm{p}) = \dfrac{R^{i+1} - R^i}{R^{i+1} + R^i}$ is the reflectivity, and $E_n^{\mathrm{av}}(\mathrm{p}) = \dfrac{E_n^i(\mathrm{p}) + E_n^{i+1}(\mathrm{p})}{2}$ is the average of normal components of the electrical field at point "p".

The average of normal components $E_n^{av}(p)$ in Eq. 3 is the sum of normal components of the electrical fields coming from primary sources, $E_n^{sr}(p)$, charges induced on horizontal boundaries between layers, $E_n^h(p)$, charges induced on cylindrical boundaries, $E_n^c(p)$, and charges coming from cylindrical electrodes of the device, $E_n^s(p)$, calculated at point "p".

Thus we have:

$$E_n^{av}(p) = E_n^{sr}(p) + E_n^h(p) + E_n^c(p) + E_n^s(p) . \tag{4}$$

Individual normal components can be calculated in the following way

$$E_n^{sr}(p) = \frac{1}{4\pi} \frac{I_A R_m(\overline{L}_{Ap}, \overline{n})}{L_{Ap}^3} , \tag{5}$$

$$E_n^h(p) = \frac{1}{4\pi\varepsilon_0} \int_{\Omega^h} \frac{\sigma^h(q) \cdot (\overline{L}_{qp}, \overline{n})}{L_{qp}^3} d\Omega^h , \tag{6}$$

$$E_n^c(p) = \frac{1}{4\pi\varepsilon_0} \int_{\Omega^c} \frac{\sigma^c(q) \cdot (\overline{L}_{qp}, \overline{n})}{L_{qp}^3} d\Omega^c , \tag{7}$$

$$E_n^s(p) = \frac{1}{4\pi\varepsilon_0} \int_{\Omega^s} \frac{\sigma^s(q) \cdot (\overline{L}_{qp}, \overline{n})}{L_{qp}^3} d\Omega^s , \tag{8}$$

where $\overline{L}_{qp}$ is the distance vector between points "p" and "q" (Fig. 1); $\overline{L}_{Ap}$ is the distance vector between points "A" and "p" (Fig. 1); $\overline{n}$ is the normal unit
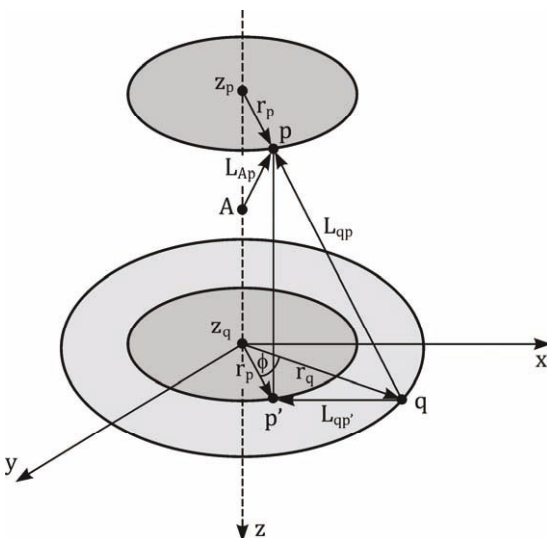

Fig. 1. Diagram of symbols.

vector to the boundary between two media; $(*,*)$ are scalar products; $\sigma^h(\mathrm{p})$, $\sigma^c(\mathrm{p})$, and $\sigma^s(\mathrm{p})$ are charge densities on the horizontal and cylindrical boundaries and the cylindrical surfaces of the electrodes of the device; I_A is current strength of the point source located at point A; and R_m is the borehole mud resistivity at point A.

Integration is held for all boundary surfaces, *i.e.*, the horizontal Ω^h, the cylindrical Ω^c, and the device Ω^s.

Putting Eqs. 6-8 into Eq. 3 we obtain Fredholm's equation of the second kind (Alpin *et al.* 1985):

$$\sigma(\mathrm{p}) - \lambda \int_{\Omega^q} N(\mathrm{p,q})\sigma(\mathrm{q})\,d\Omega^q = f(\mathrm{p}) \,, \tag{9}$$

where

$$N(\mathrm{p,q}) = \frac{K(\mathrm{p})\left(\overline{L}_{qp},\overline{n}_p\right)}{L_{qp}^3} \,, \tag{10}$$

$$f(\mathrm{p}) = 2\varepsilon_0 K(\mathrm{p}) E^{sr}(\mathrm{p}) \,, \tag{11}$$

$$\lambda = \frac{1}{2\pi} \,. \tag{12}$$

After taking into account the meanings of symbols from Fig. 1, relation 3 in cylindrical coordinate system assumes the following forms:

❑ for charge density on cylindrical boundaries:

$$
\begin{aligned}
\sigma_{n,s}^c(\mathrm{p}) = \frac{K_n^c(\mathrm{p})}{2\pi}\Bigg\{ & \frac{I_A R_m (r_n - r_A)}{\left[(r_n + r_A)^2 + (z_{np} - z_A)^2\right]^{3/2}} + \\
& + \sum_l r_l \int_{z_l^c}^{z_{l+1}^c}\int_0^{2\pi} \frac{(r_n - r_l\cos\varphi)}{\left[r_n^2 + r_l^2 + (z_{np} - z)^2 - 2r_n r_l\cos\varphi\right]^{3/2}}\sigma_l^c(z)\,dz\,d\varphi + \\
& + \sum_m \int_{r_m}^{\infty}\int_0^{2\pi} \frac{(r_n - r\cos\varphi)}{\left[r_n^2 + r^2 + (z_{np} - z_m)^2 - 2r_n r\cos\varphi\right]^{3/2}}\sigma_m^h(r)\,r\,dr\,d\varphi + \\
& + \sum_s r_s \int_{z_s^c}^{z_{s+1}^c}\int_0^{2\pi} \frac{(r_n - r_s\cos\varphi)}{\left[r_n^2 + r_s^2 + (z_{np} - z)^2 - 2r_n r_s\cos\varphi\right]^{3/2}}\sigma_s^c(z)\,dz\,d\varphi + \\
& + \sum_s \frac{I_s}{2\pi h_s} \int_{z_s^c}^{z_{s+1}^c}\int_0^{2\pi} \frac{r_n - r_s\cos\varphi}{\left[r_n^2 + r_s^2 + (z_{np} - z)^2 - 2r_n r_s\cos\varphi\right]^{3/2}}\Bigg\} \,,
\end{aligned}
\tag{13}
$$

❑ for charge density on horizontal boundaries:

$$
\sigma_m^h(\text{p}) = \frac{K_m^h(\text{p})}{2\pi} \left\{ \frac{I_\text{A} R_\text{A}(z_m - z_\text{A})}{\left[(r_{mp} + r_\text{A})^2 + (z_m - z_\text{A})^2 \right]^{3/2}} + \right.
$$

$$
+ \sum_l r_l \int_{z_l^c}^{z_{l+1}^c} \int_0^{2\pi} \frac{z_m - z}{\left[r_{mp}^2 + r_l^2 + (z_m - z)^2 - 2r_{mp}r_l \cos\varphi \right]^{3/2}} \sigma_l^c(z)\,dz\,d\varphi +
$$

$$
+ \sum_k (z_m - z_k) \int_{r_k}^{\infty} \int_0^{2\pi} \frac{1}{\left[r_{mp}^2 + r^2 + (z_m - z_k)^2 - 2rr_{mp} \cos\varphi \right]^{3/2}} \sigma_k^h(r)\,r\,dr\,d\varphi +
$$

$$
+ \sum_s r_s \int_{z_s^c}^{z_{s+1}^c} \int_0^{2\pi} \frac{z_m - z}{\left[r_{mp}^2 + r_s^2 + (z_m - z)^2 - 2r_{mp}r_s \cos\varphi \right]^{3/2}} \sigma_s^c(z)\,dz\,d\varphi +
$$

$$
+ \sum_s \frac{I_s}{2\pi h_s} \int_{z_s^c}^{z_{s+1}^c} \int_0^{2\pi} \frac{z_m - z}{\left[r_{mp}^2 + r_s^2 + (z_m - z)^2 - 2r_{mp}r_s \cos\varphi \right]^{3/2}} dz\,d\varphi \right\}, \qquad (14)
$$

where $\sigma_n^c(\text{p})$, $\sigma_1^c(z)$, $\sigma_s^c(z)$, and $\sigma_m^h(r)$ are charge densities on cylindrical boundaries of numbers n, l, s, m at points "p", "r", "z" and on horizontal boundaries of numbers m at points "r"; n – number of cylindrical boundaries; s – number of the cylinders of the device; m – number of horizontal boundaries; $K_n^c(\text{p})$, $K_s^c(\text{p})$, and $K_m^h(\text{p})$ are reflectivities at point "p" on the cylindrical boundaries of numbers n and s and on the horizontal boundary of number m; I_A and I_s are strength of current flowing from electrode A and the cylindrical electrode of the device of number s; R_m – resistivity of the mud, r_A – radial distance of point electrode A from the borehole centre; z_A – z-coordinate of point electrode A; r_n, r_l, and r_s are radial distances of cylindrical boundaries of numbers n and l and cylindrical electrode of the device of number s; z_1^c and z_{l+1}^c – z-coordinate of the start and the end of the l-th cylindrical boundary; z_s^c and z_{s+1}^c – z-coordinate of the start and the end of the s-th cylindrical electrode of the device; z_{np} – z-coordinate of the point "p" laying on the cylindrical boundary of number n; r_{mp} – radial distance of the point "p" laying on the horizontal boundary of number m; r_m – radial distance of the start of the horizontal boundary of number m; z_m – z-coordinate of the horizontal boundary of number m; and h_s – the length of the s-th cylinder of the device.

The above integral equations were solved in a numerical way. The unknown functions of charge densities were expanded into Taylor's series up to the second order. The first and second derivatives were calculated using

approximations of the finite differences. The coefficients for numerical quadratures were calculated in an analytical way, integrating kernels of integrals with elements of Taylor's series expansion. Some integrals could not be calculated in an analytical way. There were integrals of the following type:

$$L_1 = \int_0^{\pi/2} \Big[\ln \big| 1 - k^2 \sin^2 \varphi + a \big| \Big] d\varphi \ , \tag{15}$$

$$L_2 = \int_0^{\pi/2} \Big[\sin^2 \varphi \ln \big| 1 - k^2 \sin^2 \varphi + a \big| \Big] d\varphi \tag{16}$$

for $k^2 < 1$.

In those cases they were calculated numerically using the 32-point Gaussian quadrature.

After reordering the above equations, we obtain a system of linear equations with unknown charge densities of elementary cylinders and rings (Eq. 17).

$$\sum_{k=1}^{n^h} \sum_{j=1}^{n_k^h} a_{i,j}^h \cdot \sigma_j^h + \sum_{k=1}^{n^c} \sum_{j=1}^{n_k^c} a_{i,j}^c \cdot \sigma_j^c + \sum_{k=1}^{n^s} \sum_{j=1}^{n_k^s} a_{i,j}^s \cdot \sigma_j^s = f_i \ , \tag{17}$$

where $i = 1, 2, 3, \ldots, N$; $N = \sum_{k=1}^{n^h} n_k^h + \sum_{k=1}^{n^c} n_k^c + \sum_{k=1}^{n^s} n_k^s$ is the total number of all elementary cylinders and rings; $\sigma_i^{h,c,s}$ is the charge density of the i-th elementary cylinder (c), ring (h), and cylinder of the electrode of the device (s); $a_{i,j}^h$ are quadrature coefficients for horizontal boundaries; $a_{i,j}^c$ are quadrature coefficients for cylindrical boundaries; $a_{i,j}^s$ are quadrature coefficients for cylindrical electrodes of the device; n^h number of horizontal boundaries; n_k^h is the number of elementary rings on the k-th horizontal boundary; n^c is the number of cylindrical boundaries; n_k^c is the number of elementary cylinders on the k-th cylindrical boundary; n^s is the number of cylindrical electrodes of the device; n_k^s is the number of elementary cylinders on the k-th cylindrical electrode of the device; and f_i is the charge density on the i-th element due to primary sources.

Figure 2 shows the division of the cylindrical boundary into elementary cylinders of height equal to h as well as the division of the horizontal boundary for elementary coaxial rings of width initially equal to h and next increasing in a geometric progression. Unknowns in the system of linear equations (Eq. 17) are charge densities on elementary cylinders on cylindrical boundaries and cylindrical electrodes of the device as well as on elementary rings on horizontal boundaries.
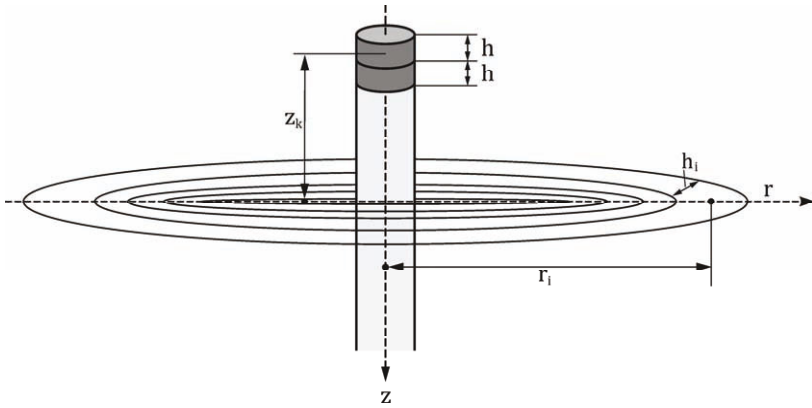
Fig. 2. Diagram of the division of cylindrical and horizontal boundaries for elementary cylinders and rings.

After putting in order, the system of linear equations (Eq. 17) can be written in the matrix form:

$$A\sigma = f \; , \tag{18}$$

where A is the matrix of coefficients, σ is the vector of unknowns, $i.e.$, charge densities on all elementary cylinders and rings, and f is the vector of free terms.

This system of linear equations was solved using the Gauss elimination method.

The potential $V(r_0, z_0)$ at any point r_0, z_0 coming from the point source and charges of elementary cylinders and rings is calculated in the following way:

$$V(r_0, z_0) = \frac{1}{4\pi} \frac{I_A R_m (z_0 - z_A)}{\left[(r_0 + r_A)^2 + (z_0 - z_A)^2 \right]^{1/2}} +$$

$$\frac{1}{4\pi\varepsilon_0} \left\{ \sum_l r_l \int_{z_l^c}^{z_{l+1}^c} \int_0^{2\pi} \frac{1}{\left[r_0^2 + r_l^2 + (z_0 - z)^2 - 2r_0 r_l \cos\varphi \right]^{1/2}} \sigma_l^c(z) dz d\varphi + \right.$$

$$+ \sum_k \int_{r_k}^{\infty} \int_0^{2\pi} \frac{1}{\left[r_0^2 + r^2 + (z_0 - z_k)^2 - 2rr_0 \cos\varphi \right]^{1/2}} \sigma_k^h(r) r dr d\varphi +$$

$$\left. + \sum_s r_s \int_{z_s^c}^{z_{s+1}^c} \int_0^{2\pi} \frac{1}{\left[r_0^2 + r_s^2 + (z_0 - z)^2 - 2r_0 r_s \cos\varphi \right]^{1/2}} \sigma_s^c(z) dz d\varphi \right\} . \tag{19}$$

The meaning of symbols is the same as in Eq. 14.

The apparent resistivity $R_a(r = 0, z_0)$ measured by probe in the middle of the borehole at the point of z-coordinate equal to z_0 is given by the following expression:

$$R_a(0, z_0) = KN \frac{V(0, z_0)}{I_A} \, , \tag{20}$$

where $KN = 4\pi L$ is the device coefficient for electric normal probe, L is the length of the device, *i.e.*, the distance between the source and the measuring electrode of the device, z_0 is the z-coordinate of the source electrode A, and I_A is the current strength flowing out from the source electrode.

In case of a lateral device, the apparent resistivity is given by the following expression:

$$R_a\left(0, z_0\right) = KL \frac{|\Delta V|}{I_A} = \frac{|V(0, M) - V(0, N)|}{I_A} \, . \tag{21}$$

In this case KL has the form:

$$KL = 4\pi \frac{AM \cdot AN}{MN} \, , \tag{22}$$

where AM and AN are distances between source electrode A and measuring electrodes M and N, respectively; z_0 is the middle of points M and N; $V(0, M)$ is the potential at the point $(0, M)$; $V(0, N)$ is the potential at the point $(0, N)$.

3. COMPARING RESULTS OBTAINED USING THE METHOD OF COULOMB CHARGES WITH ANALYTICAL SOLUTIONS

In order to test the accuracy and effectiveness of the Coulomb charges method, the apparent resistivity of a point current source lateral device was calculated. The rock formation was vertically homogeneous containing a borehole, the invaded zone, and the virgin zone. The scheme of this model is presented in Fig. 3.

At the axis of the borehole, at point A, there is the source with current strength I_A. This source and the charges induced at two cylindrical boundaries generate potential difference $V_M - V_N$ between points M and N of z-coordinates z_M and z_N. At the point $(0, z_0)$, where z_0 is the z-coordinate of the middle between points M and N, we can calculate the apparent resistivity $R_a(0, z_0)$ according to Eq. 21. Analytical solutions for such a model were presented by Dachnov (1967).

Inside the cylinder of length L_{cyl} there are two cylindrical boundaries with radii r_i and r_t, respectively, separating the mud from the invaded zone and the invaded zone from the virgin zone. Resistivities of the mud, invaded
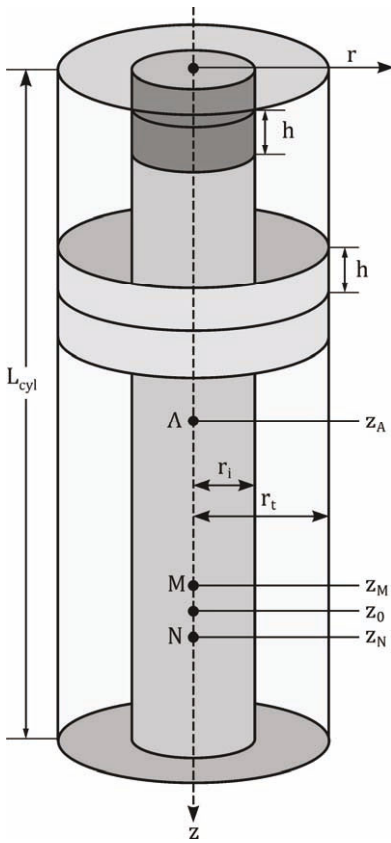
Fig. 3. Model of the rock formation.

zone and virgin zone are R_m, R^i, and R^{i+1}, respectively. Each of these cylinders with length L_{cyl} was divided into N elementary cylinders with height h, where $N = L_{cyl}/h$. Thus, the number of elementary cylinders on which the source of the current generates charge density is equal to $2N$. These charge densities are obtained by solving the system of linear equations (Eq. 18).

We calculate the potential $V(0, z_M)$ at point M in the following way:

$$V_M = V(0, z_M) = \frac{1}{4\pi} \frac{I_A R_m}{|z_M - Z_A|}$$

$$+ \frac{1}{2\varepsilon_0} \left[r_i \sum_{j=1}^{N} \sigma_j \int_{z_j - \frac{h}{2}}^{z_j + \frac{h}{2}} \frac{dz}{\left[r_i^2 + (z - z_M)^2 \right]^{1/2}} + r_t \sum_{k=1}^{N} \sigma_k \int_{z_k - \frac{h}{2}}^{z_k + \frac{h}{2}} \frac{dz}{\left[r_t^2 + (z - z_M)^2 \right]^{1/2}} \right], \quad (23)$$

where σ_j are charge densities of elementary cylinders on the boundary between mud and the invaded zone, z_j are z-coordinates of the middle of the j-th elementary cylinder on the boundary between mud and the invaded

zone, σ_k are charge densities of elementary cylinders on the boundary between the invaded zone and the virgin zone, z_k are z-coordinates of the middle of the k-th elementary cylinder on the boundary between the invaded zone and the virgin zone.

The meaning of the other symbols is explained in Fig. 3 or was mentioned earlier.

In the same way we calculate the potential $V(0, z_N)$ at point N.

Using Eq. 21 the apparent resistivity $R_a(0, z_0)$ was calculated for different values of parameters R_i/R_m, R_t/R_m, and D/d, where $d = 2r_i$ is the diameter of the borehole, $D = 2r_t$ is the diameter of the invaded zone.

Calculations were carried out for different values of the parameter L/d, where $L = |z_A - z_0|$ is the distance from the source electrode to the middle point of M and N measuring electrodes.

Calculations were made for $d = 0.2$ m, $h = 0.05$ m, $L_{cyl} = 50$ m and MN distance equal to 0.01 m.

For such values, the number of unknowns in the system of linear equations (Eq. 18) was equal to 2000. The relative error for all the results presented below for different values of parameters R_i/R_m, R_t/R_m, and D/d was less than 2%.
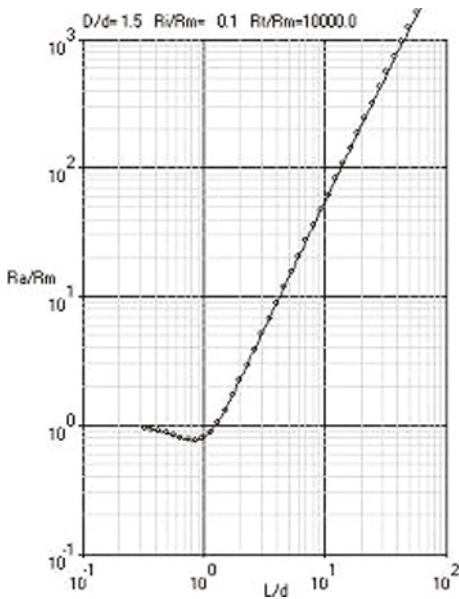

Fig. 4. Comparison of numerical results with analytical solutions for $D/d = 1.5$ $R_i/R_m = 0.1$ $R_t/R_m = 10\,000$.
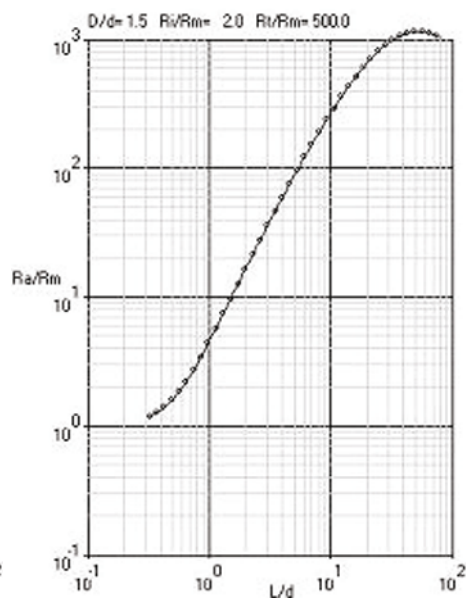
Fig. 5. Comparison of numerical results with analytical solutions for $D/d = 1.5$ $R_i/R_m = 2$ $R_t/R_m = 500$.
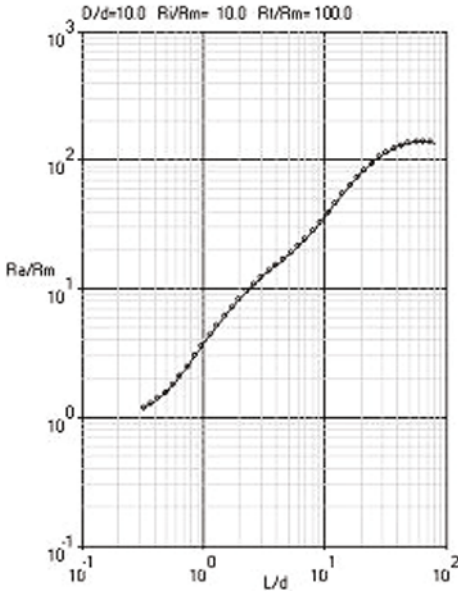
Fig. 6. Comparison of numerical results with analytical solutions for $D/d = 10$ $R_i/R_m = 10$ $R_t/R_m = 100$.
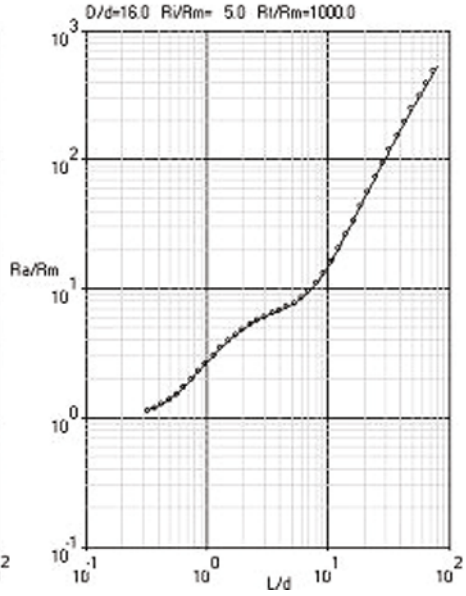

Fig. 7. Comparison of numerical results with analytical solutions for $D/d = 16$ $R_i/R_m = 5$ $R_t/R_m = 1000$.
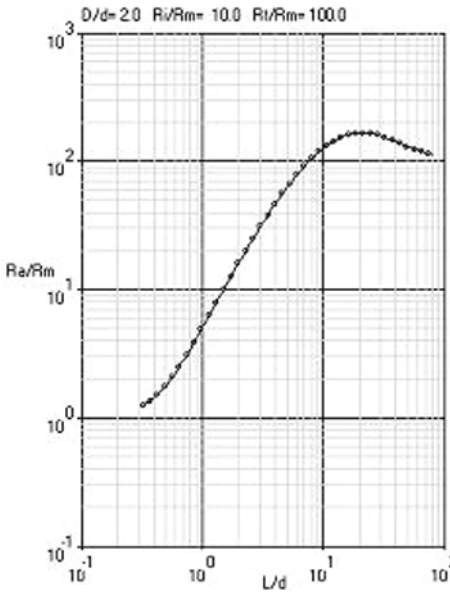

Fig. 8. Comparison of numerical results with analytical solutions for $D/d = 2$ $R_i/R_m = 10$ $R_t/R_m = 100$.
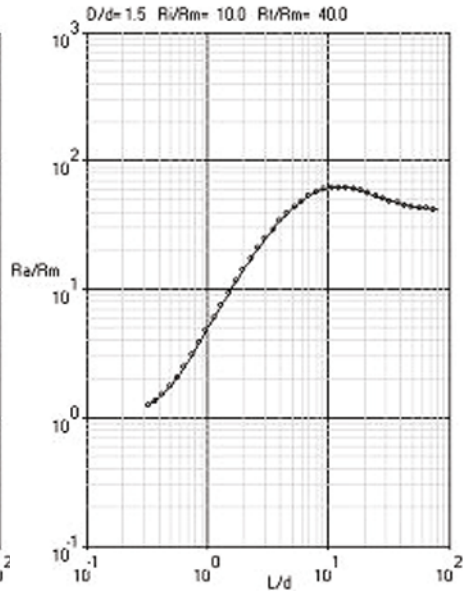

Fig. 9. Comparison of numerical results with analytical solutions for $D/d = 1.5$ $R_i/R_m = 10$ $R_t/R_m = 40$.

Increasing the length of the cylinder L_{cyl} and decreasing the height of the elementary cylinder h improved the accuracy of calculations (the relative error was less than 1%) but significantly increased the number of unknowns and, of course, the time of calculations.

The results using Coulomb charges method (points) in comparison with analytical solutions (continuous line; Dachnov 1967) for several chosen values of parameters R_i/R_m, R_t/R_m, and D/d, are presented in Figs. 4 to 9.

4. CONCLUSIONS

The Coulomb charges method presented in this paper can be used for modeling measurements of apparent resistivity carried out in a borehole with the invaded zone in multilayered rock formations. The method is effective because it does not require calculations with the use of powerful computers. A comparison of the results of calculations with analytical solutions shows that the method is also accurate. It can be successfully used for modeling measurements of apparent resistivity with the use of a more complicated construction, for instance of laterolog type.

R e f e r e n c e s

Alpin, L.M. (1964), Some theoretical methods for solving direct resistivity logging problem, *Izv. AN SSSR Ser. Geophys.* **2**, 236-238 (in Russian).

Alpin, L.M., D.S. Dajev, and A.D. Karinskij (1985), *The Theory of Alternating Fields for Exploratory Geophysics*, Niedra, Moskva (in Russian).

Dachnov, V.N. (1967), *Electric and Magnetic Methods for Logging*, Niedra, Moskva (in Russian).

Tan, M.-J., J. Gao, X.-C. Wang, and S.-Y. Zhang (2011), Numerical simulation of the dual laterolog for carbonate cave reservoirs and response characteristics, *Appl. Geophys.* **8**, 1, 79-85, DOI: 10.1007/s11770-011-0268-2.